STEM CELLS AND DEVELOPMENT 17:29–39 (2008)

DOI: 10.1089/scd.2007.0085

Original Research Report

Combinatorial Signaling Microenvironments for Studying Stem Cell Fate

CHRISTOPHER J. FLAIM,[1] DAYU TENG,[1] SHU CHIEN,[1] and SANGEETA N. BHATIA[2]

ABSTRACT

Extracellular matrix (ECM) and growth factor signaling networks are known to interact in a complex manner. Therefore, reductionist approaches that test the cellular response to individual ECM components and growth factors cannot be used to predict the response to more complex mixtures without knowledge of the underlying signaling network. To address this challenge, we have developed a technology platform to experimentally probe the interactions of ECM components and soluble growth factors on stem cell fate. We present a multiwell microarray platform that allows 1200 simultaneous experiments on 240 unique signaling environments. Mixtures of extracellular matrix (fibronectin, laminin, collagen I, collagen III, collagen IV) are arrayed using a robotic spotter and arranged in a multiwell format. Embryonic stem (ES) cells adhere to ECM spots and are cultured in mixtures of soluble factors [wnt3a, activin A, bone morphogenetic protein-4 (BMP-4), and fibroblast growth factor-4 (FGF-4)]. Differentiation along the cardiac lineage is monitored by myosin heavy chain-α-green fluorescent protein (MHCα-GFP) reporter expression as compared to growth by monitoring nuclear DNA, and both signals are quantified using a confocal microarray scanner. In developing the platform, we characterized the amount of deposited protein, the fluorescent readout of GFP expression and DNA content, and the use of a laser-based scanner as compared to fluorescent microscopy for data acquisition. The effects of growth factors on growth and differentiation are consistent with previously reported literature, and preliminary evidence of interactive signaling is illuminated. This versatile technique is compatible with virtually any set of insoluble and soluble cues, leverages existing software and hardware, and represents a step toward developing the 'systems biology' of stem cells.

INTRODUCTION

EXTRACELLULAR MATRIX (ECM) and growth factor signaling environments are part of the natural mechanisms for regulating stem cell fate. These microenvironmental stimuli are processed through a veritable web of intracellular signaling pathways. Evidence to date suggests that interactions between these pathways are critical in determining cell fate, yet are often difficult to predict from experiments using simple signaling environments in vitro. For example, growth factor signaling responses can be diminished in the absence of integrin binding [1,2]. In turn, integrin binding can alter the dynamics of growth factor signal transduction events at multiple points along the mitogen-activated protein (MAP) kinase pathway [3] and can even transactivate growth factor receptor pathways [4]. In combination, ligation of both integrins and growth factor receptors can result in a per-

[1]Departments of Bioengineering and Medicine, University of California-San Diego, La Jolla, CA 92093-0412.

[2]Health Sciences and Technology/Electrical Engineering & Computer Science, Massachusetts Institute of Technology, Cambridge, MA 02139 and Department of Medicine, Brigham & Women's Hospital, Boston, MA 02115.

The work reported here was presented as Flaim et al., "Combinatorial signaling microenvironments for manipulating cell fate," at the California Tissue Engineering meeting, September 15, 2006.

sistent and strong activation of the MAP kinase pathway [1,5]. Given the complex crosstalk elucidated thus far, stem cell differentiation may be best explored in the context of interacting ECM and growth factor signaling [6,7].

Recent studies using conventional methodology, such as quantitative western blots, have provided a glimpse of the startling complexity revealed from studying even small sets of ECM and growth factor environments [8–10]. Furthermore, statistical methodology for identifying cross-talk in large data sets is an area of active research [7]. The interest in signaling crosstalk naturally encompasses more than just stem cell fate control. Indeed, a host of applications, such as culture media/environment optimization for cell growth and bioproduction, rely on identifying complex signaling environments. However, conventional cell culture methodology cannot easily meet the demands for increased throughput, mandating the need for novel platforms that enable the systematic probing of complex signaling environments in parallel. In particular, the quantity and cost of purified ECM and growth factor required, compounded by the increased workload of manipulating large numbers of cell culture wells, are problematic. To sidestep these problems, we and others have developed microarray-based, "parallel" culture platforms that deposit nanoliter quantities of materials using automated robotic spotters [11–15]. Our own studies initially focused on the effects of combinatorial ECM signaling (i.e,. interactions between ECM stimuli) on primary adult somatic cells and stem cell populations by using epifluorescent microscopy to assess effects on cell fate after several days in culture; however, despite the ability to vary the insoluble microenvironment in this platform, all cells were exposed to similar soluble stimuli (i.e., a single medium formulation). Here, we sought to extend this platform to incorporate exposure to multiple soluble growth factor environments by incorporating robotic spotting into a multiwell platform where each well contains multiple ECM spots in the context of a different soluble environment (see Fig. 1, below).

The ECM microarray significantly simplifies the task of high-throughput cell culture through parallelization, yet has still been reliant thus far on serial data acquisition through epifluorescent microscopy. Therefore, we sought to explore whether one could leverage DNA microarray scanners to speed data collection and analysis. To this end, we have further adapted our previous ECM microarray technology to convert cell fate 'readouts' such as green fluorescent protein (GFP) reporter activity and DNA content to fluorescent wavelengths compatible with confocal laser scanner hardware and software found in DNA microarray scanners.

In this report, we first present the quantitative validation of the platform. As a demonstration of its utility, we then apply it to the study of mouse embryonic stem (mES) cell differentiation toward the cardiac lineage in response to 240 unique ECM and growth factor signaling environments, with multiple replicates of each condition. The effects of growth factors on growth and cardiac lineage differentiation are consistent with previously reported literature, and preliminary evidence of interactive growth factor–, ECM–growth factor, and ECM–ECM signaling is illuminated.

MATERIALS AND METHODS

ECM array slide preparation

Glass slide cleaning. Glass microscope slides (75 mm × 25 mm × 1 mm, Corning) were cleaned with detergent followed by five complete rinses in deionized water (dH_2O). After washing in fresh Millipore water (18 M-ohm/cm^2, MQH_2O), slides were washed with 100% acetone, 100% methanol, and finally with five rinses of MQH_2O. The slides were next etched in 0.05 N NaOH solution for 1 h, followed by thorough MQH_2O rinsing. Slides were dried with filtered compressed air and then further dried in a vacuum oven for 1 h.

Silanization. Slides were functionalized in a 2% solution of 3-(trimethoxysilyl)propyl methacrylate (Sigma) in anhydrous toluene over 1 h, rinsed in toluene, dried with compressed air, and baked for 15 min in a vacuum oven.

Acrylamide gel pad fabrication. Stock solutions of acrylamide/bis-acrylamide and photo initiator were prepared as follows. A solution of 10.55% acrylamide and 0.55% bis-acrylamide was prepared in MQH_2O. A 10× photo-initiator stock of I2959 was prepared at 200 mg/ml in 100% methanol. The working polymer solution consisted of 10% acrylamide, 0.5% bis-acrylamide in a 90% MQH_2O, and 10% methanol diluent. Then 40 μl of the prepolymer solution was placed on the silanized slide and covered with a 22 mm × 22 mm #2 coverslip resulting in an ~80-μm-thick layer. The slide was next exposed to 365-nm ultraviolet A light (UVA) (~1.5 mW/cm^2) for 10 min and then immersed in MQH_2O.

ECM array fabrication

Protein printing buffer. 2X protein printing buffer consisted of 200 mM acetate (Sigma S2889), 10 mM EDTA, 40% glycerol, 0.5% triton X-100 in MQH_2O, pH adjusted to 4.9 using glacial acetic acid.

ECM protein preparation and mixing. Purified ECM stock solutions were prepared at 1 mg/ml (rat collagen I, human collagen III, mouse laminin, mouse collagen IV, human fibronectin) and stored appropriately. ECM stock proteins were diluted 50:50 with 2X printing buffer, mixed, and loaded into a 384-well polypropylene source plate (Greiner).

ECM arraying. SMP 3.0 spotting pins (Telechem) were prepared by oxalic acid treatment according to manufacturer's directions. Slides were prepared by dehydration on a 40°C hotplate for 15 min. All printing was done with a SpotArray 24 (Perkin Elmer) using the recommended motion-control parameters (Telechem) at room temperature with humidity controlled

to ~65% RH. Each of the 20 ECM mixtures was deposited with five replicates at a 450-μm pitch. After printing, ECM arrays were stored at 4°C in a sealed box containing a slurry of NaCl for ~48 h.

Multiwell ECM array culture

The multiwell ECM array format was prepared for cell culture as follows. The FAST-Frame carrier and well/gasket structures (Whatman) were cleaned with detergent, rinsed in water, and stored in 70% ethanol until 24 h before use. After overnight soaking in sterile dH_2O, the FAST-frame and well structures were exposed to UVC germicidal (254 nm) radiation in a sterile flow hood for 5 min on each side followed by assembly of the well structure on the FAST-frame.

mES cell culture

mES cells were propagated in an undifferentiated state on gelatinized flasks in a 5% CO_2 incubator according to standard practices. Culture medium consisted of Knockout-Dulbecco's modified Eagle medium (KO-DMEM; Gibco) supplemented with 12.5% ES-screened fetal bovine serum (FBS; Hyclone), 2 mM L-glutamine, 1× nonessential amino acids, and 2-mercaptoethanol. Leukemia inhibitory factor (LIF; ESGRO) was added to culture media at 1,000 U/ml during undifferentiated expansion. Cell culture medium was changed daily, and the cells were passaged every 2 days (~80% confluency). Cells were seeded on multiwell ECM array substrates at approximately 750,000 cells/ml in ES medium without LIF at 100 μl per well. Cells were cultured for 18 h before changing to differentiation medium or fixation. The I114 mES β-galactosidase reporter cell line was donated by Dr. Lesley Forrester. The myosin heavy chain-α-green fluorescent protein (MHC-α-GFP) reporter mES cells were provided by Dr. Mark Mercola (The Burnham Institute).

The basal differentiation medium consisted of KO-DMEM supplemented with 4% ES-screened FBS, 2 mM L-glutamine, 1× nonessential amino acids, 10 mM HEPES, 100 U/ml penicillin/streptomycin, 200 ng/ml heparin, and 2-mercaptoethanol. The four growth factors, when present in a mixture, were at the following concentrations: wnt3a, 100 ng/ml; activin A, 30 ng/ml; BMP-4, 30 ng/ml; FGF-4, 60 ng/ml. Purified soluble wnt3a was obtained from Dr. Karl Willert (UCSD Human Stem Cell Core). Its activity was confirmed by the ability to stimulate a wnt-responsive GFP-reporter 293 cell line (gift of Dr. Karl Willert). Activin A, bone morphogenetic protein-4 (BMP-4), and fibroblast growth factor-4 (FGF-4) were obtained from R&D Systems.

Slide staining and preparation

For ECM characterization, slides were stained with Sypro Ruby (Probes) solution overnight on orbital shaker. The slides were then destained with 10% methanol and 7% acetic acid solution and then air dried in the dark. Slides were imaged using a Scanarray 4000 with 546-nm laser excitation (90% power) and a 617-nm emission filter (PMT voltage 80%) and quantified using GenePix software.

Multiwell ECM array culture slides were prepared as follows to retain natural GFP fluorescence [16] and to retain cell spots firmly attached to the gel support. Culture wells were disassembled and slides were placed in quadriPERM cell culture vessels (Sigma). The cultured ECM-array slides were rinsed briefly in cold Hanks' balanced salt solution (HBSS) (with Ca^{2+} and Mg^{2+}) containing 10 mM HEPES, and then fixed in a multistep procedure. The fixative was a chilled 4% paraformaldehyde solution prepared freshly in 150 mM phosphate buffer, pH 7.2. Slides were fixed for 5 min at 4°C, followed by 10 min at room temperature. Cells were then washed in HBSS, transferred to −20°C methanol as a secondary fixation step, and washed in cold HBSS before storage at 4°C.

Immediately before staining, cells were permeabilized in 0.1% Triton X-100 in phosphate-buffered saline (PBS), and blocked in 3% bovine serum albumin (BSA), 50 mM glycine in Tris-EDTA buffer, pH 8.0, at room temperature. The ECM array slides were then reassembled with FAST-frame wells for the antibody and nucleic acid staining procedures. All washes and staining steps were performed using 100 μl of volume per well, with continuous agitation on an orbital shaker. After a brief rinse with 1% BSA/PBS, slides were treated with a polyclonal rabbit anti-GFP-Alexafluor 647 conjugated antibody at room temperature (Probes, diluted to 1 μg/ml in 1% BSA PBS). Nucleic acids were stained using a 200-nM solution of POPO-3 (Probes, Cy3 wavelength emission, diluted in PBS) at room temperature. When indicated, cells were stained in a 0.001% Hoechst 33258 (Probes) water solution.

For preparations where natural GFP fluorescence was of importance, the samples were equilibrated for 15 min with a mounting medium consisting of 50% glycerol in a Tris-EDTA buffer adjusted to pH 8.5 [17]. The slides were then removed from the FAST-frame, an 18 mm × 18 mm #1 coverslip was applied, and the preparation was sealed using Cytoseal 60. For longer-term preservation and antifade protection, slides were instead mounted in ProLong Gold antifade with DAPI (Probes), cured at room temperature for 48 h on a flat surface in the dark, and finally sealed with Cytoseal 60.

Imaging and quantification

Where indicated, microscope images of each well-array area were acquired at 10× using an Olympus IX81 motorized microscope equipped with a Prior Proscan stage, ORCA-ER 12-bit cooled-CCD camera (Hammamatsu), and an image acquisition journal written in Metamorph 6.2r3 (Universal Imaging). The well arrays were imaged using phase-contrast, Hoechst, GFP, Cy3, and Cy5 optics at 56 stage positions, which were subsequently montaged.

For most quantification purposes, the slides were imaged using a confocal DNA microarray scanner (Scanarray 4000) at 5-μm pixel resolution. The POPO-3 nucleic acid stain (similar to Cy3 spectra) was imaged using a 543-nm laser excitation and 570-nm emission filter (42% laser power, PMT voltage 70%). The Alexafluor 647 (Cy5-equivalent) "antibody-converted GFP signal" was imaged using a 633-nm excitation laser and 670-nm emission filter (laser power 78%, PMT voltage 70%). Each well array (4.5 mm × 4.5 mm) was imaged using a focus height that gave the maximum signal for each channel at the center of the array.

Both the microscope montaged images and the microarray

scanner images were quantified using GenePix Software. Array features were autoaligned according to the nominal array feature size and dimension. Incorrectly identified spots were either manually adjusted or flagged for removal. Only spots where >70% of the pixels were above the local background on both channels were used during subsequent analysis.

Data analysis

We used the local background subtracted median signal value for each cell island (or "spot" in DNA microarray terminology) in the subsequent processing. For each spot, we calculated the $\log_2$ ratio of the GFP signal/nucleic acid signal. GFP and DNA data were also $\log_2$ transformed prior to analysis. To estimate the effects of ECM, growth factor, and interactions between these factors, we performed a factorial analysis on all collected data [18]. The statistical analysis was performed using Minitab v.15 (Minitab Inc., PA). GFP/DNA, GFP, and DNA effect magnitudes were calculated using a model containing all one- and two-factor interaction terms. The statistical significance of each effect was estimated using analysis of variance (ANOVA).

RESULTS

Multiwell ECM microarrays

The assembled platform consists of four standard microscope slides on a standard multiplate footprint compatible with 96-well spacing on manual and automatic fluid handlers. Each 1 × 3-inch slide houses 16 wells separated by a removable silicone gasket in which 12 wells were spotted with identical arrays of 100 ECM spots, resulting in 4,800 spots per platform (Fig. 1). We first characterized the ECM protein deposition on two slides (24 wells, each containing complete ECM microarrays) by SYPRO Ruby protein staining and detection by confocal microarray laser scanner (ex, 546 nm; em, 617 nm). A representative fluorescent image of a single well is shown in Fig. 2A. Quantitative analysis showed consistent protein deposition between replicate spots within each array (Fig. 2B). Increases in the number of spotted ECM components resulted in approximately linear increases in fluorescent signal (not shown). mES cells attached to the spotted ECM components as previously reported, creating uniformly sized cellular microarrays atop differing ECM mixtures [12] (Fig. 2C).

Quantitative in situ assays

We next set out to validate the in situ quantitative assay for GFP reporter activity. In addition, we sought to convert the GFP signal to a Cy5-equivalent signal that would be compatible with a laser confocal scanner with an excitation wavelength of approximately 635 nm. For this purpose, we created cellular calibration arrays from predefined mixtures of constitutively expressing EYFP mouse ES cells and nonfluorescent ES cells. All arrays were seeded with the same total cell number but in differing ratios; a 1:1 mixture (EYFP:nonfluorescent), 1:4 and 1:16. A 0:1 mixture was included to evaluate background staining. After 18 h of culture, cells were fixed, stained with a Alexaflour 647-labeled anti-GFP antibody and Hoechst, and mounted. As expected, on the basis of the sequence homology of GFP and enhanced yellow fluorescent protein (EYFP), we found that the anti-GFP antibody cross-reacted with EYFP. Each well was then imaged by epifluorescent microscopy at 10× magnification at 56 stage positions using the following filters: Hoechst, GFP, Cy3, and Cy5. None of the Cy3 wavelength images showed appreciable fluorescence nor did unstained EYFP-expressing cells in the Cy5 wavelength images (data not shown). In contrast, antibody-converted EYFP cell mixtures did exhibit Cy5 staining that qualitatively reproduced the EYFP signal. For example, the average GFP signal and the Alexa 647 converted signal from a cell array decreased as the proportion of EYFP cells in the mixture decreased. Figure 3 A and B, illustrates this phenomenon in montaged images of Hoechst, GFP, and Cy5 channels at both low (10×) and high (inset) magnification for 1:1 and 1:16 mixtures, respectively.

Having qualitatively validated the conversion of fluorescent protein expression to the Alexa 647 signal, we sought to characterize the calibration arrays quantitatively. To accomplish this, montaged microarray images acquired by microscopy at each wavelength (Hoechst, GFP, Cy5) were processed using DNA microarray feature extraction and quantification techniques (GenePix Pro). Spot measurements were excluded from further analysis if either wavelength had <70% of the pixels above the local background. For each population mixture, we plotted the extracted feature data for GFP versus Hoechst and Alexa 647 versus Hoechst (Fig. 3A,B, bottom panels). For the Alexa 647-converted signal against DNA data, all Pearson coefficients were ≥0.731 ($p < 0.001$), indicating a strong positive linear correlation (data not shown). For GFP data, all Pearson coefficients were ≥0.685 ($p \leq 0.001$). Linear regression was used to determine the slope of a best-fit line for each data set (in all cases $r^2 > 0.9$). As expected, increased nuclear staining corresponded positively with increased fluorescent signal for both GFP and Alexa 647 and the slope of the relation was dependent on the fraction of fluorescent cells in the mixture. Slope ratios for four-fold mixture dilutions were very close to the expected value of 1/4 for both sets of fluorescent data (GFP and converted, Alexa 647, data not shown).

To illustrate the quantitative abilities of the platform more clearly, we normalized each GFP and Alexa 647 spot measurement to the corresponding Hoechst measurement, and plotted the data against the relative dilu-

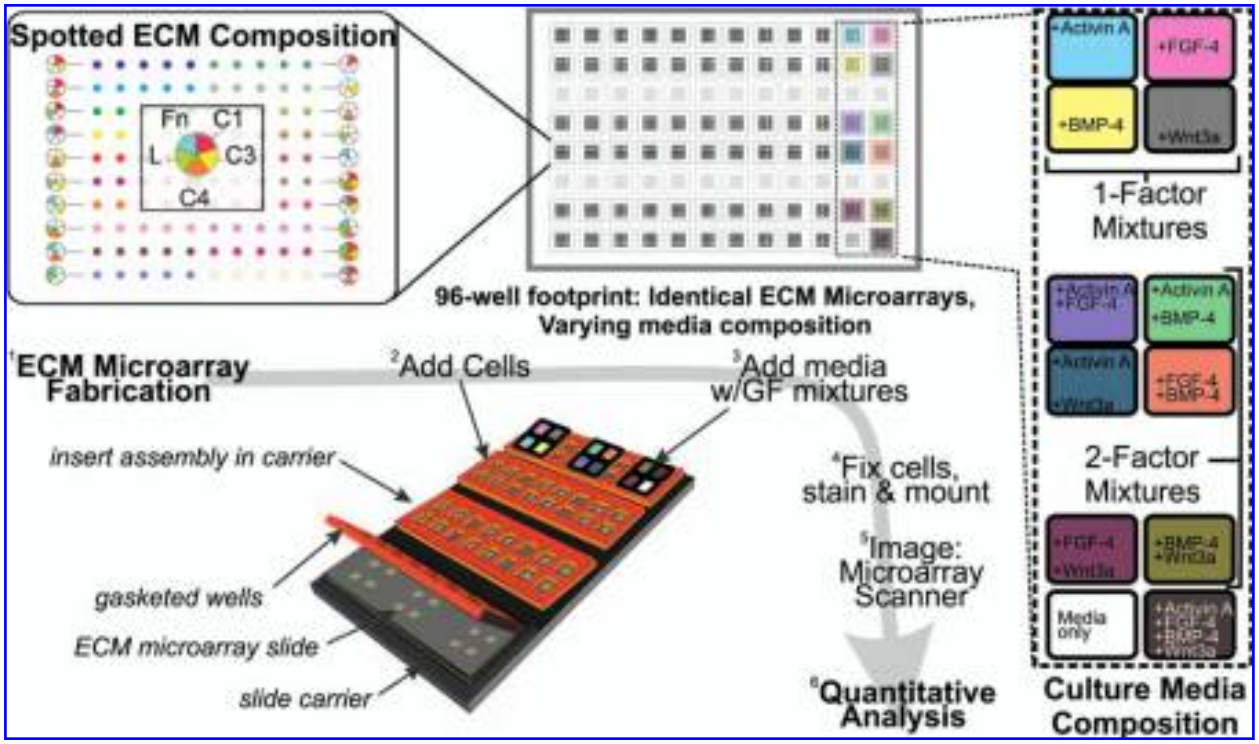

FIG. 1. Multiwell ECM microarray. Multiwell plate (*top middle*) in which each well accommodates a unique medium composition over an array of 100 ECM spots. Cells were seeded atop 20 spotted mixtures of ECM in five replicates each as specified in the upper-left legend, included collagen I, human collagen III, mouse collagen IV, mouse laminin, and human fibronectin. Each well was exposed to medium containing a combination of growth factors (*right*). Here, we tested 12 different mixtures of four growth factors known to affect cardiac lineage differentiation (activin A, FGF-4, BMP-4, Wnt3A) as shown at right. Multiwell ECM arrays were created by assembling gasketed well structures on the printed arrays (*bottom middle*). The diameter and spacing of the wells conformed to a 96-well footprint. ES cells in suspension were seeded on the arrays where they attach only to the ECM protein domains. After microarray formation, medium with various soluble growth factors was added during the differentiation period. The slides were then processed for staining, mounted, and imaged using either a microscope or a DNA slide scanner. Resultant images were quantified using DNA microarray feature extraction software and analyzed.

tion factor (Fig. 3C). The normalized GFP and Alexa 647 data had Pearson coefficients of 0.923 and 0.81 respectively ($p < 0.001$); however, the variance also increased (data not shown). After applying a $\log_2$ transformation, the data had approximately equal variance. Pearson coefficients for the transformed data were 0.918 and 0.930, respectively ($p < 0.001$). Linear regression of all normalized GFP data versus relative cell concentration indicated a slope of 1.88 ($r^2 = 0.876$). Similar analysis of normalized Alexa 647 data indicated a slope of 3.01 ($r^2 = 0.901$). Thus, the GFP reporter activity could be transformed to generate quantitative, linear relationships over the dynamic range of interest.

Validation of confocal microarray scanner imaging

Quantitative imaging of cells using a confocal laser scanner required the development and validation of appropriate procedures. Test scans suggested that the measured intensity dropped to 80% of the maximum value when the laser focal position was shifted by ~10 μm from the optimum (data not shown). Measurements taken from multiple gel-pad slides indicated that the optimum focus position varied by as much as 100 μm across an entire slide. However, variations within each subarray (~4 mm × 4 mm) were sufficiently small. Thus, we empirically determined the optimum focus position for each subarray before scanning. For quantitative data comparison, the calibration arrays were reimaged on a confocal microarray scanner at 5-μm resolution. Cy3-wavelength scans of these samples did not reveal detectable signals (data not shown), whereas the Cy5 array scans yielded nearly identical results compared to microscope images (Fig. 3D).

Cardiac lineage differentiation of mES cells

mES cells containing an MHCα-GFP reporter were next cultured in 12 separate wells. Each well contained

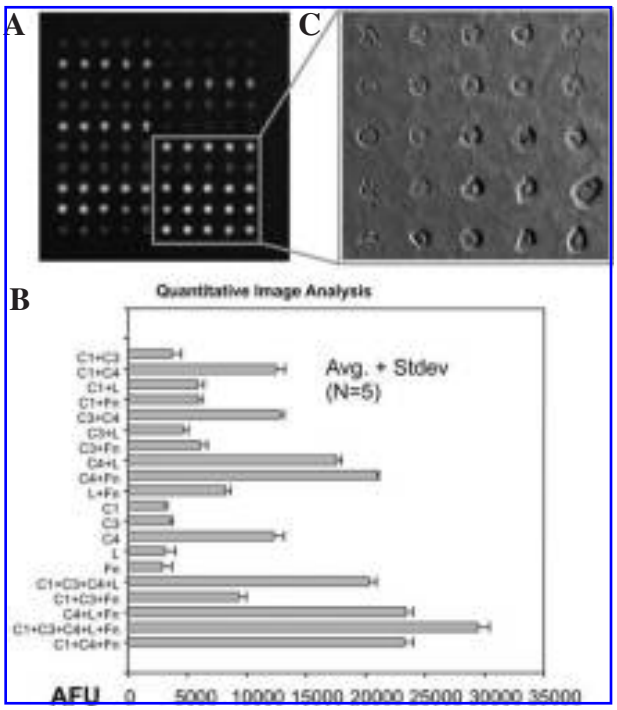

FIG. 2. Multiwell ECM microarray characterization. (**A**) Fluorescent image of SYPRO Ruby protein stained ECM microarray. Layout of ECM mixtures is specified in Fig. 1. (**B**) Quantitative image analysis of protein deposition in ECM microarrays in arbitrary fluorescent units acquired by confocal laser microarray scanner. (**C**) The addition of ES cells yields adherent colonies of 150 μm diameter upon the ECM microarray. Scale bar, 450 μm.

a nominally identical ECM microarray cultured in a unique mixture of soluble wnt3a, activin A, BMP-4, and FGF-4, as summarized in Fig. 1. These factors have been implicated in embryonic cardiac lineage specification [19]. GFP (assessed using Alexa 647 dye conversion on the Cy5 channel) and DNA (assessed using POPO-3 DNA dye on the Cy3 channel) were quantified at 18 h (just before the addition of solublegrowth factors) and 48 h after the addition of growth factor mixtures. For the quantification that follows, we adopted a conservative approach, only using data where both Cy3 and Cy5 channel measurements were statistically above local background levels. Of the 1,800 ECM array features interrogated for this experiment, 939 (~50%) satisfied our conservative criteria. Eight 18-h arrays (four, dual stained; two, DNA only; and two, unstained) were quantified, yielding 152, 112, and 52 usable measurements, respectively. The 48-h differentiated slide yielded 623 usable measurements of the 1,200 possible data points. Cell arrays fixed at 18 h showed a low level of GFP activity (data not shown). Microarrays stained with POPO-3, a Cy3-equivalent DNA dye, did not exhibit appreciable signals on the unstained Cy5 channel, and completely unstained arrays had minimal signals on both Cy3 and Cy5 scans (data not shown).

Differentiation efficiency, the fraction of cells in a population undergoing differentiation, is a metric of interest for stem cells. In light of this, we calculated the GFP/DNA signal ratio as an estimate of differentiation efficiency, and plotted it against the DNA signal as an estimate of cell number. Figure 4A presents all of the data using this transformation. Data from the 18-h arrays cluster in three distinct locations, representing dual-stained, DNA-only, and unstained cell populations. Data from the 48-h differentiated arrays form a fourth cluster, only slightly overlapping with the 18-h data. Scatter plots of MHCα differentiation efficiency under different soluble environments at 48 h versus total DNA content (Fig. 4B) indicated that most growth factor mixtures induced a heterogeneous response. Viewed as an ensemble, the data are consistent with the "growth versus differentiation" paradigm wherein colonies with higher DNA content exhibit a predominance of mitotic activity over reporter activity, resulting in a lower differentiation efficiency score.

To analyze the effects observed using this platform and compare them with previously published data, we performed a factorial analysis of the $\log_2$-transformed GFP/DNA, GFP, and DNA data. The model included all one- and two-factor terms. Figure 5A presents the effect magnitudes for all single-factor effects and their statistical significance. Of the effects calculated for growth factors, we noted that the addition of wnt3a correlated with decreased differentiation efficiency and GFP levels (Fig. 5A). Conversely, activin A and BMP-4 stimulation produced a modest increase in GFP levels, consistent with previous reports on the role of activin A and BMP-4 in promoting cardiogenesis [19], and the inhibition of wnt signaling in promoting cardiac differentiation [20].

Aside from the outcomes induced by ECM and growth factor individually, such data can potentially be used to uncover putative crosstalk between signaling pathways. As an example, we plotted the two-factor interaction effect magnitudes in a similar manner (Fig. 5B). In the realm of ECM–ECM crosstalk, collagen I and collagen III correlated individually with decreased differentiation efficiency whereas simultaneous stimulation correlated with a significantly positive effect on differentiation efficiency (Fig. 5B). Because this effect was dominated by a decrease in DNA content, simultaneous stimulation may have predominantly impacted cell survival. Collagen I and fibronectin also exhibited an antagonistic interaction effect. In the realm of growth factor–growth factor crosstalk, activin A and BMP-4 exhibited the strongest interaction effect by negatively impacting differentiation efficiency, though this effect may simply be additive rather than synergistic. In contrast, wnt3a and activin A each negatively influenced differentiation efficiency

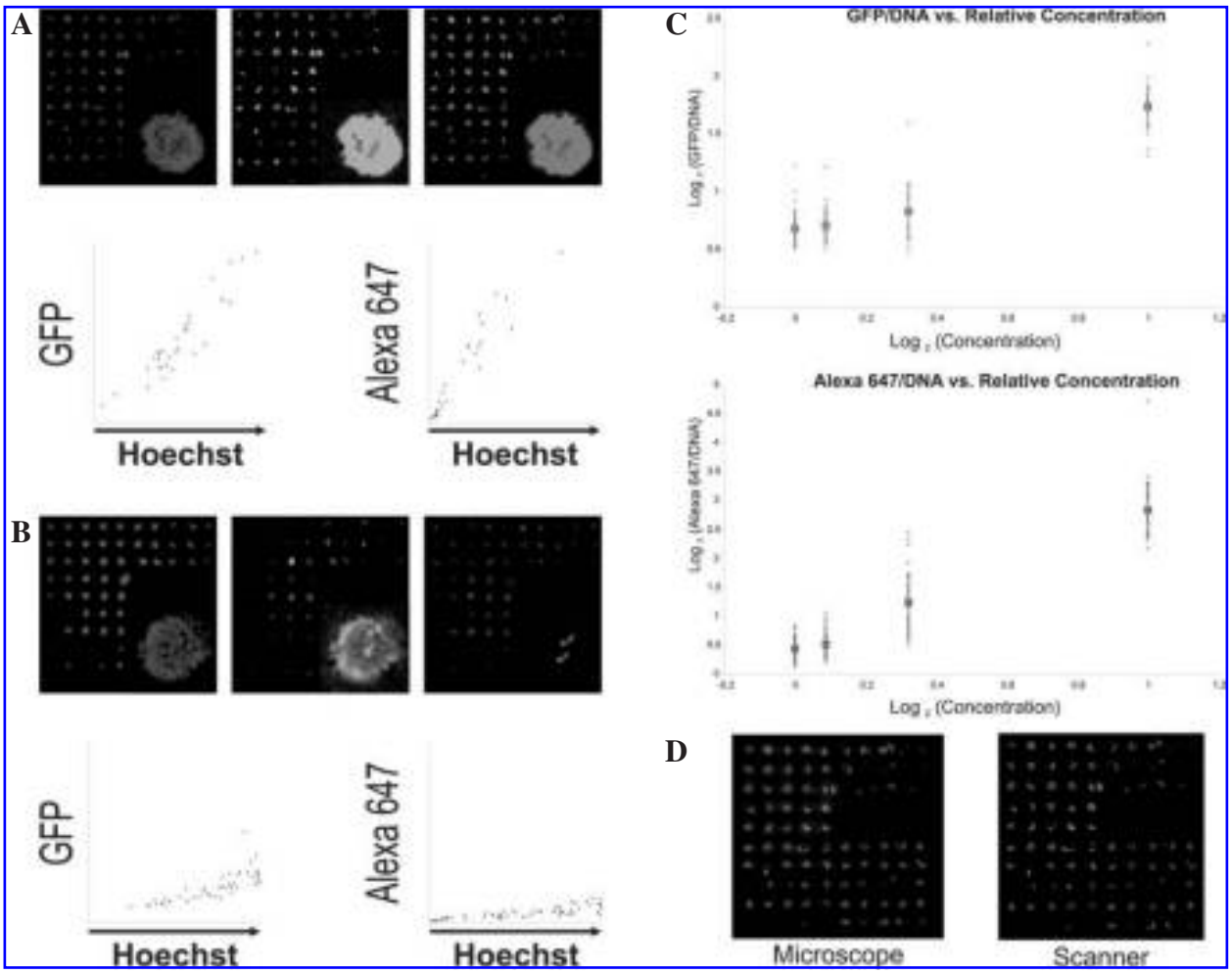

FIG. 3. Validation of GFP conversion and characterization of quantitative assays. (**A**) Calibration arrays were constructed by mixing populations of fluorescent ES cells with wild-type cells. Mixtures of cells were seeded on arrays in varying ratios. (**A**) A 1:1 mixture of cells imaged by microsocopy at three wavelengths (Hoechst, GFP, Alexafluor 647). (*Inset images*) Magnified view of the same cell island. Alexa 647 images appear qualitatively to mirror GFP fluorescence. Scatter plots of quantitative data extracted from images (*lower panel*). Each data point represents the signal from a single cell island. In all cases, GFP and Alexa 647 data were linearly related to the Hoechst signal from the same island. (**B**) A 1:16 mixture of fluorescent to nonfluorescent cells. GFP (and Alexa 647) fluorescence decreased as the proportion of fluorescent cells in the population mixture decreased. In scatter plots, the slope of the scatter trend decreased as the population mixture changed with a decrease in the proportion of fluorescent cells. (**C**) Ratio of GFP fluorescence to DNA fluorescence (*top*) and converted (Alexa 647 to DNA) (*bottom*) plotted against cell number (the mixture ratio of fluorescent to nonfluorescent cells). The $\log_2$-transformed data showed similar variance at each relative cell concentration, and a linear trend with $r^2 = \sim 0.9$ in both cases. The box symbol indicates the average, and error bars indicate standard deviation. (**D**) Qualitative correlation of montaged microscopy image of Alexa 647 (*left*) and laser confocal scanner (*right*).

when presented alone but increased differentiation efficiency when presented simultaneously (Fig. 5B). In the realm of ECM–growth factor crosstalk, we noted that fibronectin exhibited antagonistic interactions with wnt3a and activin A. Individually, the components show negative effects on differentiation efficiency, whereas they had a positive effect when presented in combination (Fig. 5B). Collagen I and BMP-4 also displayed apparently antagonistic effects.

DISCUSSION

To investigate the interactions between growth factor and ECM stimuli on stem cell differentiation in a high-throughput format, we adapted our previously published ECM microarray platform [12] to a multiwell format and developed quantitative assays for cell fate that are compatible with confocal laser microarray scanner hardware and software for data acquisition. As a case study, we in-

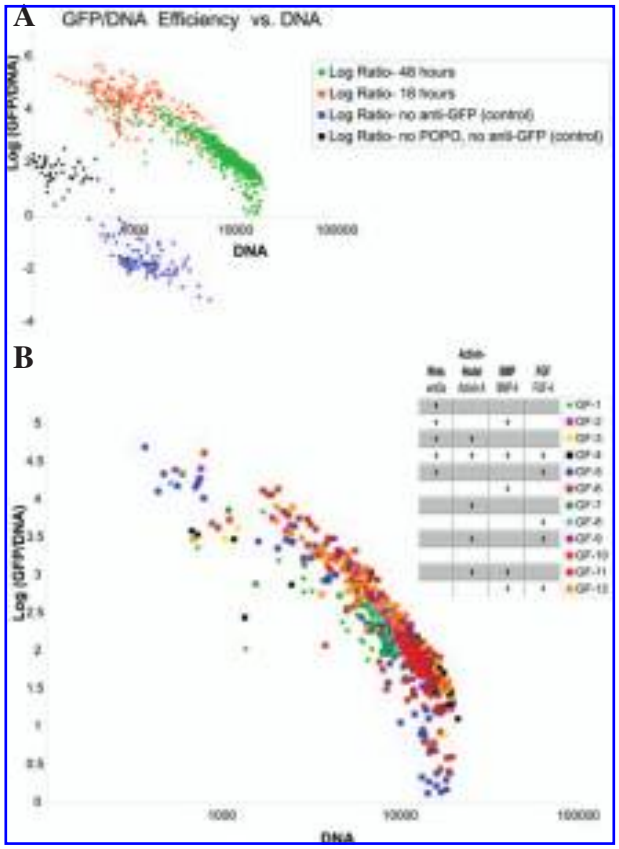

FIG. 4. "Differentiation efficiency" scatter plots. mES cells were seeded in the multiwell ECM microarray format as in Fig. 1, cultured for various times under differing stimuli and assayed for MHC-α reporter activity by conversion of GFP signal to Alexa 647 (**A**). Aggregated data for "differentiation efficiency" scored by ratio of GFP fluorescence to total DNA (i.e., reporter activity normalized per number of cells) plotted against total DNA for controls, 18-h and 48-htime points. (**B**) "Differentiation efficiency" for ES cells cultured for 48 h under different growth factor stimulation. + indicates the presence of a growth factor in the media.

vestigated the differentiation efficiency of ES cells along the cardiac lineage over 48 h in 240 unique ECM and growth factor signaling environments using an enhanced green fluorescent protein (EGFP) reporter driven by the expression of MHCα. Recently, Soen et al. [14] developed a similar platform that instead presents soluble cues (morphogens and cytokines) in an immobilized format to adult neural precursor cells and used microscopy for data acquisition. The platform presented here has the comparative advantage of presenting soluble cues in a soluble, rather than insoluble, form, which is recognized as critical to the cellular response at the expense of array density (i.e., without the need for gaskets to form wells, higher-density arrays theoretically can be achieved). Presentation of soluble cues in the soluble form also enables test medium formulations for ES cell culture to be tested easily, which may be an important practical application of this technology. In addition, the use of laser confocal microarray scanners and software, rather than microscopy and image analysis, to process low-resolution cellular responses used in this study (e.g., average GFP expression) increases throughput by 10-fold or more in our hands. We believe this eases the dissemination of cellular microarray technologies given the widespread use of laser confocal microarray scanners.

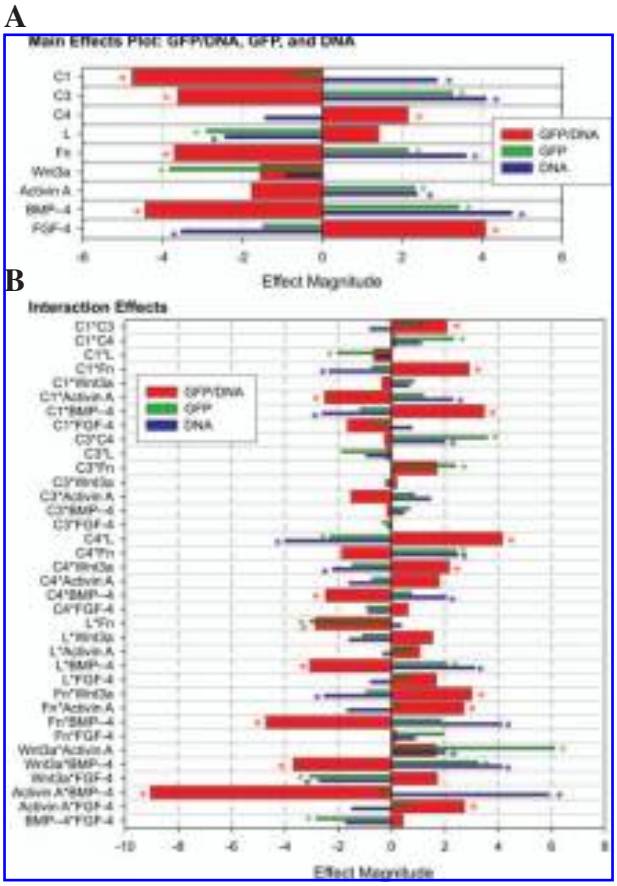

FIG. 5. Multivariate analysis of growth factor and ECM signaling. The effects of ECM and growth factor components on converted GFP signal (green bar, a metric of reporter activity), DNA signal (blue bar, a metric of cell number), and GFP/DNA (red bar, a metric of "differentiation efficiency"). The effect magnitude is calculated using factorial analysis. Further details on this statistical approach for multivariate analysis are described in the methods. An asterisk (*) indicates $p < 0.05$ for the indicated colored bar. (**A**) Plot of coefficient magnitude for individual stimuli. Wnt3a shows a negative effect on GFP levels, whereas BMP-4 and activin A show a positive effect that is consistent with reported literature. (**B**) Interaction effects of paired stimuli. Examples of potential crosstalk signatures present in this data are highlighted in the text. Such data sets combined with appropriate analysis algorithms could be used to generate hypotheses for more in-depth studies.

Assay development

We sought to develop a quantitative method of measuring GFP expression and DNA content in situ. Although GFP is a powerful biological tool, it presented potential problems in light of our experimental goals. In principle, a GFP signal could be measured without conversion to another fluorophore using a DNA microarray scanner; however, by convention, most scanners are equipped only with excitation lasers and optics for Cy3- and Cy5-wavelength dyes. GFP fluorescence is also influenced by multiple environmental factors, including pH, oxidation, and protein conformation, and is not as stable or bright as other organic dyes [17]. In addition, cellular autofluorescence can be particularly bright in the green wavelengths, especially in the case of dead or dying cells. These considerations motivated our exploration of a dye-conversion strategy.

To explore simultaneously the dye-conversion strategy and characterize the quantitative nature of the proposed methods, we prepared calibration cellular arrays using controlled mixtures of mES cells that constitutively express EYFP and wild-type mES cells. EYFP cells were used purely for convenience rather than EGFP; however, this approximation proved adequate for our purposes due to the overlapping spectra and sequence homology of the two fluorescent proteins. Specifically, EYFP was detectable using GFP microscopy optics and could be labeled using anti-GFP antibody. Using the calibration arrays, microscopy for data acquisition, and microarray software for data analysis, we found: (1) a linear correlation between DNA and GFP staining in pure populations of EYFP cells, (2) stepwise decreasing slopes of the linear correlation when populations were mixed with wild type (nonfluorescent cells), and (3) quantitative equivalence of the antibody-converted GFP signal from GFP to Alexa 647. To develop a calibration curve for each fluorescent species, we performed a log transformation of the raw data to meet Gaussian statistical criteria (normal distribution and equal variance). Subsequently, calibration curves were generated for both GFP and Alexa 647 with r^2 values of approximately 0.9, providing further evidence that a linear correlation could be generated over the dynamic range of interest.

Next, we considered alternatives to microscopic data acquisition because microscopic imaging of an entire slide at multiple wavelengths can require several hours to complete. Cognizant that DNA microarray scanners are more commonly available than automated fluorescent microscopes and that they can acquire images in only 10 min, we sought to adapt our platform further. The tradeoff we considered in adapting the platform to a confocal scanner was in imaging resolution—typically no better than 5 μm for a confocal scanner as compared to submicron resolution for microscopy. Our experience suggested that sub-micron resolution cell array images would not provide an appreciable benefit for our application of interest, which was scoring differentiation efficiency. mES cells typically grew at high densities on the microarrays and often in a three-dimensional manner that would pose significant challenges to subcellular-level image segmentation algorithms. Instead, we adopted a population-based approach to quantitation by leveraging microarray software to derive an average signal from each ECM spot with its small population of cells. Although low-resolution images do not generally provide adequate spatial information to localize individual nuclei, the quantitative information content for the population average is virtually the same. To demonstrate this, we digitally down-sampled microscope cell array images to 5-μm resolution, and then to 10-, 20-, and 50-μm resolutions. Quantitative analysis of these "simulated" image resolutions yielded virtually identical results (data not shown). As a final validation, we scanned the arrays presented in Fig. 4. Quantitative data analysis from these images exhibited linear correlations similar to those discussed above (GFP vs. DNA) and was of comparable quality (data not shown).

Differentiation of mES cells along the cardiac lineage

We probed ECM components and growth factors of interest in differentiation of ES cells along the cardiac lineage by using an MHC-α reporter after 48 h of stimulation. As one would expect, our results demonstrated that the addition of most soluble growth factors correlated with increased DNA content (and presumably with increased cell number). In contrast, some matrix components, for example the presence of laminin, consistently reduced DNA content, possibly through negative effects on cell survival. Upon further inspection, two-factor data means plots (not shown) indicate that collagen IV and laminin show little effect on DNA content unless they are applied simultaneously. In the early embryo and artificial embryoid body (EB) environments, epiblast (or epiblast-like) cells survive cavitation in part due to the assembly of an underlying basement membrane [21–23]. In this light, our data may signify a recapitulation of some cavitation events, where only an epithelialized monolayer survives an apoptotic signal. Another global observation was that differentiation efficiency (GFP/DNA) increased with colonies that contained less DNA (i.e., exhibited less growth). This finding is consistent with the 'growth versus differentiation' paradigm that is often used to describe the switch between self-renewal (proliferation in an undifferentiated state) and differentiation (coordinated alteration of gene expression in the absence of proliferation).

Our case study illustrates just one application of this novel platform. We limited ourselves to a single genetic reporter at a single (early) time point; however, this technique can be easily extended to multiple reporters, different lineages, and different microenvironmental stimuli. Indeed, we have previously demonstrated that ES cell colonies grow over 5 days into tethered EB-like structures that exhibit increased differentiation efficiencies. Despite the limitations of this case study, we found that the data were consistent with reported literature and suggested that interactions between growth factor and ECM signaling pathways are at work in stem cell fate decisions.

We have developed a microarray platform for probing the effects of ECM and growth factor mixtures on stem cell differentiation through the quantification of GFP reporter expression and DNA content. We demonstrated that a DNA microarray scanner provided equivalent data to microscopy images for the intended purpose of tracking differentiation efficiency and required only a fraction of the time (~1/30). To demonstrate the effectiveness of this technology, we studied mES differentiation toward the cardiac lineage under 240 ECM and growth factor treatment conditions in five replicates. The results obtained from this technology were consistent with results reported in the literature regarding cardiogenesis, differentiation, and proliferation. Although many applications can be envisioned for this technology, we believe that the greatest benefit will be realized in combination with new bioinformatics methods and analyses [7,24]. In the future, systematic methods of generating scientific hypotheses in simple cell-based assays such as those presented here followed by validation in traditional systems will dramatically aid in the analysis of complex phenomena such as stem cell differentiation [7,25].

ACKNOWLEDGMENTS

We thank Hua Hwang and Eric Diaz (UCSD Bioengineering) for assistance with array fabrication, scanning, and data analysis; Karl Willert (UCSD Molecular Medicine) for donating soluble wnt3a and the 293-wnt reporter cell lines; Mark Mercola (The Burnham Institute) for donating the GFP-reporter ES cell line; L. Forrester (University of Edinburgh) for providing the I114 cell line; C. Largent (Cel Associates) and D. Schabacker (Argonne) for useful discussions on acrylamide gel pad fabrication; T. Martinsky (Telechem) for printing parameters; and J. Norwich (S. Chien Lab), R. Agustin (imaging, J. Price Lab), and S. Khetani (cell patterning). Funding was generously provided by the U.S. National Institutes of Health, the National Institute of Diabetes and Digestive and Kidney Diseases, the National Science Foundation's Faculty Early Career Development (CAREER) Program, and the David and Lucile Packard Foundation.

REFERENCES

1. Fashena SJ and SM Thomas. (2000). Signalling by adhesion receptors. Nature Cell Biol 2:E225–229.
2. Watt FM. (2002). Role of integrins in regulating epidermal adhesion, growth and differentiation. EMBO J 21:3919–3926.
3. Schwartz MA and MH Ginsberg. (2002). Networks and crosstalk: integrin signalling spreads. Nature Cell Biol 4:E65–E68.
4. Yamada KM and S Even-Ram. (2002). Integrin regulation of growth factor receptors. Nature Cell Biol 4:E75–E76.
5. Comoglio PM, C Boccaccio and L Trusolino. (2003). Interactions between growth factor receptors and adhesion molecules: breaking the rules. Curr Opin Cell Biol 15:565–571.
6. Sastry SK and AF Horwitz. (1996). Adhesion-growth factor interactions during differentiation: an integrated biological response. Dev Biol 180:455–467.
7. Natarajan M, K-M Lin, RC Hsueh, PC Sternweis and R Ranganathan. (2006). A global analysis of cross-talk in a mammalian cellular signalling network. Nature Cell Biol 8:571–580.
8. Prudhomme W, GQ Daley, P Zandstra and DA Lauffenburger. (2004). Multivariate proteomic analysis of murine embryonic stem cell self-renewal versus differentiation signaling. Proc Natl Acad Sci USA 101:2900–2905.
9. Prudhomme WA, KH Duggar and DA Lauffenburger. (2004). Cell population dynamics model for deconvolution of murine embryonic stem cell self-renewal and differentiation responses to cytokines and extracellular matrix. Biotechnol Bioeng 88:264–272.
10. Woolf PJ, W Prudhomme, L Daheron, GQ Daley and DA Lauffenburger. (2005). Bayesian analysis of signaling networks governing embryonic stem cell fate decisions. Bioinformatics 21:741–753.
11. Anderson DG, S Levenberg and R Langer. (2004). Nanoliter-scale synthesis of arrayed biomaterials and application to human embryonic stem cells. Nature Biotechnol 22: 863–866.
12. Flaim CJ, S Chien and SN Bhatia. (2005). An extracellular matrix microarray for probing cellular differentiation. Nature Methods 2:119–125.
13. Kuschel C, H Steuer, AN Maurer, B Kanzok, R Stoop and B Angres. (2006). Cell adhesion profiling using extracellular matrix protein microarrays. Biotechniques 40:523–531.
14. Soen Y, A Mori, TD Palmer and PO Brown. (2006). Exploring the regulation of human neural precursor cell differentiation using arrays of signaling microenvironments. Mol Syst Biol 2:E1–E14.
15. Nakajima M, T Ishimuro, K Kato, IK Ko, I Hirata, Y Arima and H Iwata. (2007). Combinatorial protein display for the cell-based screening of biomaterials that direct neural stem cell differentiation. Biomaterials 28:1048–1060.

16. Brock P, IHL Mamelars and TM Jovin. (1999). Comparison of fixation protocols for adherent cultured cells applied to a GFP fusion protein of the epidermal growth factor receptor. Cytometry 35:353–362.
17. Chalfie M and SR Kain, eds. *Green Fluorescent Protein: Properties, Applications, and Protocols*. (2006). Wiley-Interscience, Hoboken, NJ.
18. Box G, W Hunter and J Hunter. *Statistics for Experimenters*. (1978). Wiley, New York.
19. Foley A and M Mercola. (2004). Heart induction: Embryology to cardiomyocyte regeneration. Trends Cardiovasc Med 14:121–125.
20. Foley AC and M Mercola. (2005). Heart induction by Wnt antagonists depends on the homeodomain transcription factor Hex. Genes Dev 19:387–396.
21. Li X, Y Chen, S Scheele, E Arman, R Haffner-Krausz, P Ekblom and P Lonai. (2001). Fibroblast growth factor signaling and basement membrane assembly are connected during epithelial morphogenesis of the embryoid body. J Cell Biol 153:811–822.
22. Coucouvanis E and GR Martin. (1999). BMP signaling plays a role in visceral endoderm differentiation and cavitation in the early mouse embryo. Development 126:535–546.
23. Esner M, J Pachernik, A Hampl and P Dvorak. (2002). Targeted disruption of fibroblast growth factor receptor-1 blocks maturation of visceral endoderm and cavitation in mouse embryoid bodies. Int J Dev Biol 46:817–825.
24. Kato T, K Tsuda and K Asai. (2005). Selective integration of multiple biological data for supervised network inference. Bioinformatics:bti339.
25. Tegner J, MKS Yeung, J Hasty and JJ Collins. (2003). Reverse engineering gene networks: Integrating genetic perturbations with dynamical modeling. Proc Natl Acad Sci USA 100:5944–5949.

Address reprint requests to:
Dr. Sangeeta N. Bhatia
Health Sciences and Technology/
Electrical Engineering & Computer Science
Massachusetts Intitute of Technology
77 Massachusetts Avenue, Building E19-502D
Cambridge, MA 02139

E-mail: sbhatia@mit.edu

Received for publication May 9, 2007; accepted June 5, 2007.